Article

Not peer-reviewed version

Transcriptomic Profiling of Heat-Treated Oriental Lily Reveals *LhERF109* as a Positive Regulator in Anthocyanin Accumulation

Mei Zhou , Lijia Zeng , Fan Li , Chunlian Jin , Jungang Zhu , Xue Yong , Mengxi Wu , Beibei Jiang , Yin Jia , Huijuan Yuan , Jihua Wang * , Yuanzhi Pan *

Posted Date: 26 March 2025

doi: 10.20944/preprints202503.2014.v1

Keywords: Oriental lily; heat stress; transcriptome; anthocyanin biosynthesis; WGCNA; *LhERF109*

 doi:10.20944/preprints202503.2014.v1

Article

Transcriptomic Profiling of Heat-Treated Oriental Lily Reveals *LhERF109* as a Positive Regulator in Anthocyanin Accumulation

Mei Zhou [1], Lijia Zeng [1], Fan Li [2,3], Chunlian Jin [2,3], Jungang Zhu [1], Xue Yong [1], Mengxi Wu [1], Beibei Jiang [1], Yin Jia [1], Huijuan Yuan [3,4], Jihua Wang [2,3,*] and Yuanzhi Pan [5,*]

[1] College of Landscape Architecture, Sichuan Agricultural University, Chengdu, China
[2] Yunnan Seed Laboratory, Kunming, 650200, China
[3] Floriculture Research Institute, Yunnan Academy of Agricultural Sciences National Engineering Research Center for Ornamental Horticulture, Key Laboratory for Flower Breeding of Yunnan Province, Kunming, China
[4] Institute of Alpine Economics and Botany, Yunnan Academy of Agricultural sciences, Lijiang, China
[5] College of Forestry, Sichuan Agricultural University, Chengdu, China
* Correspondence: wjh0505@gmail.com (J.W.); scpyzls@163.com (Y.P.)

Abstract: Pink-flowered Oriental lily cultivars exhibit significant color fading under high temperature, but the underlying regulatory mechanisms remain unclear. We subjected Oriental lily 'Souvenir' plants to temperature treatments (20°C and 35°C) and performed transcriptome sequencing and weighted gene co-expression network analysis (WGCNA). High temperature (35°C) significantly reduced anthocyanin content in tepals. Transcriptome analysis identified 8,354 differentially expressed genes, with GO and KEGG analyses revealing a dynamic transition from early stress responses to metabolic adaptation. WGCNA revealed a module strongly correlated with anthocyanin content, from which we constructed a gene co-expression network using known anthocyanin-related genes, including the key transcription factor *LhMYB12* and structural genes involved in the anthocyanin biosynthetic pathway (*LhANS*, *LhDFR*, *LhUGT78*, and *LhF3'H*). Through this comprehensive network analysis, we successfully identified and screened *LhERF109* as a promising regulatory candidate. Functional characterization through transient overexpression of *LhERF109* enhanced anthocyanin accumulation and upregulated biosynthetic genes including *LhMYB12*, while silencing produced opposite effects. These findings identify *LhERF109* as a positive regulator of anthocyanin biosynthesis under high temperature, providing new targets for breeding heat-tolerant lilies with stable flower coloration.

Keywords: Oriental lily; heat stress; transcriptome; anthocyanin biosynthesis; WGCNA; *LhERF109*

1. Introduction

The suppression of anthocyanin biosynthesis under high temperature is a widespread phenomenon observed across the plant kingdom, affecting both fruits and ornamental flowers [1]. This temperature-sensitive response has gained increasing research attention due to global climate warming and its significant impact on horticultural industries [2].

Mounting evidence suggests that high temperature can directly impacts MYB transcription factors and influence anthocyanin accumulation through complex upstream regulatory pathways. In Oriental lilies, elevated temperatures disrupt MYB transcription factor balance by suppressing R2R3-MYB activators (*LhMYB12*) while inducing MYB repressors (*LhMYBC2*), leading to reduced expression of anthocyanin biosynthetic genes including CHS, DFR, and ANS [3,4]. Similar direct effects on MYB regulation have been documented in other species: in grape berries, high temperature significantly reduces the expression of *VvMYBA1* and *VvMYBA2* activators [5]; in apples, heat stress

 doi:10.20944/preprints202503.2014.v1

downregulates *MdMYB10* [6]; and in Arabidopsis, elevated temperatures suppress *AtPAP1*/*AtMYB75* activator expression while enhancing the repressive activity of *AtMYBL2* [7]. In *Malus* profusion, high temperatures suppress R2R3-MYB activators *(MpMYB10*) while inducing MYB repressors (*MpMYB15*), reducing expression of key anthocyanin biosynthetic genes *MpCHS*, *MpDFR*, *MpLDOX*, and *MpUFGT* [8].These examples collectively demonstrate that temperature-induced modulation of the balance between MYB activators and repressors represents a conserved regulatory mechanism affecting anthocyanin biosynthesis across diverse plant species.

In fruits and *Arabidopsis thaliana*, the mechanisms by which high temperature inhibits anthocyanin accumulation have been extensively characterized. In apple (*Malus* domestica), thermal stress modulates the expression and activity of MYB10 through the COP1-HY5 photothermal integration module [9]. The interaction between high temperature and light signaling involves B-box (BBX) transcription factors, where *MdCOL4* (BBX24) interacts with *MdHY5* to inhibit *MdMYB1* expression [10]. Similar upstream regulatory networks have been identified in Arabidopsis, and the same COP1-HY5-MYBL2 signaling module has been confirmed to regulate anthocyanin biosynthesis in response to high temperature [11,12]. In contrast to fruits and model plants, ornamental flowering crops show diverse regulatory mechanisms for anthocyanin biosynthesis under high temperatures. Some heat-tolerant cultivars maintain stable pigmentation at elevated temperatures, suggesting the HY5-COP1 module may not be the primary regulatory pathway in these species [6,13]. Instead, ornamental flowering crops exhibit more complex regulatory mechanisms involving multiple external cues (like light and hormones) that may dilute the influence of the HY5-COP1 module in controlling floral pigmentation [14–16]. Although research on upstream mechanisms of high-temperature suppression of anthocyanin synthesis is limited, studies show that MYB transcription factors, key regulators of anthocyanin biosynthesis, are regulated by various upstream factors [17–20]. Among these, APETALA2/ETHYLENE RESPONSIVE FACTOR (AP2/ERF) family members may play important roles in integrating temperature and hormone signals to control floral pigmentation. For instance, in 'Viviana' lilies (*Lilium* spp.), *LvERF113*, induced by ethylene, promotes anthocyanin synthesis in tepals by repressing the negative regulator *LvMYB1*, forming the *LvMYB5-LvERF113-LvMYB1* module under *LvMYB5*'s positive regulation[21]. Similarly, in apple (*Malus* domestica), *MdERF109* enhances fruit anthocyanin biosynthesis via methyl jasmonate (MeJA) signals, interacting with *MdWER*[22]. These examples underscore ERF's role in coordinating hormonal and environmental cues for pigmentation.

Oriental lily (*Lilium* spp., Oriental Group) is renowned for its exceptionally large, fragrant flowers with vibrant colors and distinctive recurved petals [23]. These outstanding horticultural traits establish its significant position in both cut flower industry and landscape applications [24]. As an important breeding parent, Oriental lily has been widely used in interspecific hybridization, resulting in series like LLO (Longiflorum × Oriental lily) [25] and AOA (Asiatic × Oriental lily) [26,27]. However, pink-flowered cultivars commonly exhibit heat sensitivity, with flower color fading under high temperature stress [28]. This undesirable trait is often inherited by progeny, seriously affecting product quality and economic value. Research has shown that flower color fading in Oriental lilies under high temperature is primarily regulated by MYB transcription factors, however, the upstream regulatory mechanisms remain unclear. Previous studies have identified the crucial roles of MYB transcription factors such as *LhMYB12* and *LhMYBC2* in response to high temperature, but little is known about the upstream molecular networks that regulate these MYB factors.

In this study, we performed transcriptome sequencing analysis of 'Souvenir' Oriental lily under control and high-temperature conditions, and conducted weighted gene co-expression network analysis (WGCNA) with known MYB transcription factors, anthocyanin biosynthesis structural genes, and related transcription factors to explore the upstream regulatory mechanisms of high temperature-induced color fading.

 doi:10.20944/preprints202503.2014.v1

2. Materials and Methods

2.1. Plant Materials and Temperature Treatments

Oriental lily 'Souvenir' plants at developmental St_2-St_3 were selected for uniformity and subjected to controlled temperature treatments of 20℃ (control) and 35℃ (high temperature) in growth chambers. Environmental conditions were standardized across both treatments (16h light/8h dark photoperiod, 70% relative humidity, 12,000 lx light intensity). Tepal samples were systematically collected at 12h, 24h, 48h, and 72h post-treatment (designated as T1, T2, T3, and T4, respectively), with three biological replicates per treatment combination to enable robust color measurement and physiological analyses.

2.2. Determination of Anthocyanin Content

Total anthocyanin content was measured using the pH differential method, with modifications based on Song et al. [29]. 0.5 g of finely ground tepal tissue was extracted with 5 mL of acidified methanol (0.1% HCl, v/v) for 24 h at 4°C in darkness. The extract was centrifuged at 12,000 g for 10 min at 4°C, and the supernatant was collected. Absorbance was measured at 530 nm and 657 nm using a spectrophotometer (UV-1800, Shi madzu, Japan). Total anthocyanin content was calculated as $X = (A_{530} - 0.25A_{657}) \times W \cdot g^{-1}$. where X is the total anthocyanin content (relative units), *A530* and *A645* are the absorbance values at 530 nm and 645 nm, respectively, and W is the sample weight (g). Measurements were performed in triplicate for each treatment.

For specific anthocyanin analysis, the method proposed by Xia et al. [30] was adopted, and the determination was performed using a high-performance liquid chromatography (HPLC) instrument (Shimadzu Corporation, Japan). Anthocyanins were separated on a Shim-pack Scepter C18 column (4.6 mm × 250 mm, 5 μm) at 30°C. The mobile phase consisted of (A) 0.1% formic acid and (B) acetonitrile. The gradient elution program was as follows: 0-8 min, 10-22.2% B; 18-25 min, 22.2-22.8% B; 25-28 min, 22.8-44% B; 28-45 min, 44-50% B; 45-50 min, 50-60% B; 50-70 min, 60-85% B. The flow rate was 1.0 mL/min, and the injection volume was 10μL. Cyanidin-3-O-glucoside was identified by comparing retention times and spectral characteristics with authentic standards (Shanghai yuanye), and quantified using standard curves. Each sample run for HPLC was repeated three times under the same conditions.

2.3. Determination of Sugar Content

Samples preserved in a -80 °C freezer were retrieved for the determination of sugar content. The contents of sucrose, reducing sugars, and soluble sugars were determined according to the kit protocol (G0506W, G0502W, G0501W Grace Biotechnology, Suzhou, China).

2.4. RNA Extraction and Transcriptome Sequencing

Total RNA was extracted from 'Souvenir' lily tepal samples using the Universal Plant Total RNA Extraction Kit (RC112-01, Vazyme, Nanjing, China) according to the manufacturer's instructions. RNA quality and integrity were assessed via agarose gel electrophoresis, with purity verified using a Nanodrop 2000 spectrophotometer (Thermo Fisher Scientific Inc., USA) [31]. High-quality RNA samples (OD260/280 ratio of 1.8 to 2.0) from each time point (12, 24, 48, and 72 h) with three biological replicates were used for library construction. Library preparation and RNA-Seq, performed by Biomarker Technologies (Beijing, China), involved poly(A) mRNA enrichment using oligo (dT) magnetic beads, followed by fragmentation, first and second-strand cDNA synthesis, purification (QiaQuick PCR Extraction Kit, Qiagen), end-repair, poly(A) addition, and adapter ligation. The resulting libraries were sequenced on the Illumina HiSeqTM 2000 platform using a PE150 strategy. Raw sequencing data were processed using Trimmomatic to remove adapters, reads with >10% unknown nucleotides, and low-quality sequences (base quality ≤10). Due to the lack of a reference genome for Oriental lily, de novo assembly was performed using Trinity software (v2.8.5) with

 doi:10.20944/preprints202503.2014.v1

default parameters (K-mer = 31, K-mer cover = 6 for specific runs). Candidate coding regions were identified with TransDecoder (v5.5.0), and ESTscan was used for sequences that could not be aligned. The assembled unigenes were functionally annotated via BLASTx searches (E-value ≤ $1\times e^{-5}$, identity > 70%, query coverage ≥ 80%) against multiple databases including Nr, Swiss-Prot, KEGG, GO, and COG. Additionally, protein domains were detected using InterProScan (v5.33-72.0) based on the InterPro database. Read mapping and expression quantification were performed using Bowtie2 and RSEM, respectively, with gene expression levels calculated as FPKM (fragments per kilobase of transcript per million mapped reads).

2.5. Weighted Gene Co-Expression Network Analysis (WGCNA)

Weighted gene co-expression network analysis was performed using the WGCNA package (v1.69) in R. Genes with low expression (FPKM < 1 in more than half of the samples) were filtered out before analysis. A signed network was constructed with a soft threshold power of $\beta = 12$, determined by the scale-free topology criterion. Module identification was performed using dynamic tree cutting with a minimum module size of 30 genes and a module similarity threshold of 0.25. Module-trait relationships were calculated by correlating module eigengenes with anthocyanin content data. The gene co-expression network was visualized using Cytoscape (v3.8.0) with a weight threshold of 0.95.

2.6. Phylogenetic Analysis

The full-length coding sequence of *LhERF109* was identified from the transcriptome data. Multiple sequence alignment (MSA) of ERF proteins from *Arabidopsis thaliana*, retrieved from The Arabidopsis Information Resource (TAIR) database (https://www.arabidopsis.org/) [32], was performed using MUSCLE (v3.8.31) with default parameters. The phylogenetic tree was constructed using the maximum likelihood method in MEGA 7.0 with 1,000 bootstrap replicates. The evolutionary distances were computed using the JTT matrix-based method. The tree was visualized and annotated using iTOL (Interactive Tree of Life).

2.7. Transient Transformation of Lily Tepals

For transient transformation experiments, the full-length coding sequence of *LhERF109* was amplified by PCR and cloned into the pS1300 expression vector under the control of the CaMV 35S promoter using KpnI and SalI restriction sites. For virus-induced gene silencing (VIGS), a 300-bp fragment of *LhERF109* was cloned into the pTRV2 vector. All constructs were verified by sequencing before use.

For transient expression and VIGS experiments, St_2 flower buds of Oriental lily (*Lilium* 'Souvenir') were selected based on their developmental uniformity. Whole flower branches, each bearing a single St_2 bud, were used for infiltration. Approximately 100 μL of the *Agrobacterium* suspension was injected into the abaxial side of each tepal using a 1-mL needleless syringe, ensuring even distribution of the inoculum. Post-infiltration, the entire flower branch was placed in a container with its stem inserted into sterile distilled water to maintain hydration and support the flower during the experiment. The setup was then transferred to a growth chamber under controlled conditions. The samples were initially subjected to a 12-hour dark treatment at 20°C to minimize stress, followed by culture at 20°C under a 16-hour light/8-hour dark photoperiod [33]. Tepal samples were collected 72 hours post-infiltration for phenotypic observation, anthocyanin content measurement (via spectrophotometric analysis), and gene expression analysis, including quantitative real-time PCR (qRT-PCR) to assess *LhERF109* expression levels.

2.8. Quantitative Real-Time PCR (qRT-PCR)

The quantitative expressions of crucial genes involved in anthocyanin synthesis was analyzed by qRT-PCR referring to previous description [34]. The mRNA expression level was assessed with $2^{-\triangle\triangle Ct}$ method using an internal reference gene *LhActin*.

 doi:10.20944/preprints202503.2014.v1

2.9. Statistical Analysis

All experiments were performed with at least three biological replicates. Statistical analysis was performed using SPSS software (version 25.0). Data were analyzed using Student's t-test or one-way analysis of variance (ANOVA) followed by Tukey's HSD test. Differences were considered statistically significant at $p < 0.05$. Data are presented as means ± standard deviation (SD).

3. Results

3.1. Effect of High Temperature on the Physiology and Biochemistry of Oriental Lily 'Souvenir'

Under the 20°C treatment, the St_2 (Figure 1A) of the lily 'Souvenir' exhibited a progressive petal - coloring phenomenon. In sharp contrast, upon initiating the 35℃ treatment, the red coloration of the lily petal began to decline (Figure 1B). Subsequently, this color continued to fade, eventually approaching an almost white state in the lily petals (Figure 1B). Consistent with these visual observations, the total anthocyanin content and Cyanidin 3-O-β-rutinoside content in tepals under 20°C treatment showed a continuous increase, while both decreased steadily in tepals under 35°C treatment (Figure 1C).

The determination of the changes in the sugar content of Oriental lily 'Souvenir' flowers under high temperature showed that over time, the sucrose content in the petals generally increased under suitable temperature conditions, while it generally decreased under high temperature conditions (Figure 1D).

To validate the accuracy of RNA-seq detection, this study conducted an investigation into the expression patterns of structural genes that have been firmly established to be involved in the regulation of anthocyanin synthesis. The results (Figure 1E) demonstrated congruence with those derived from the transcriptomic analysis, thereby indicating that the sequencing results obtained in this study exhibit a high level of reliability.

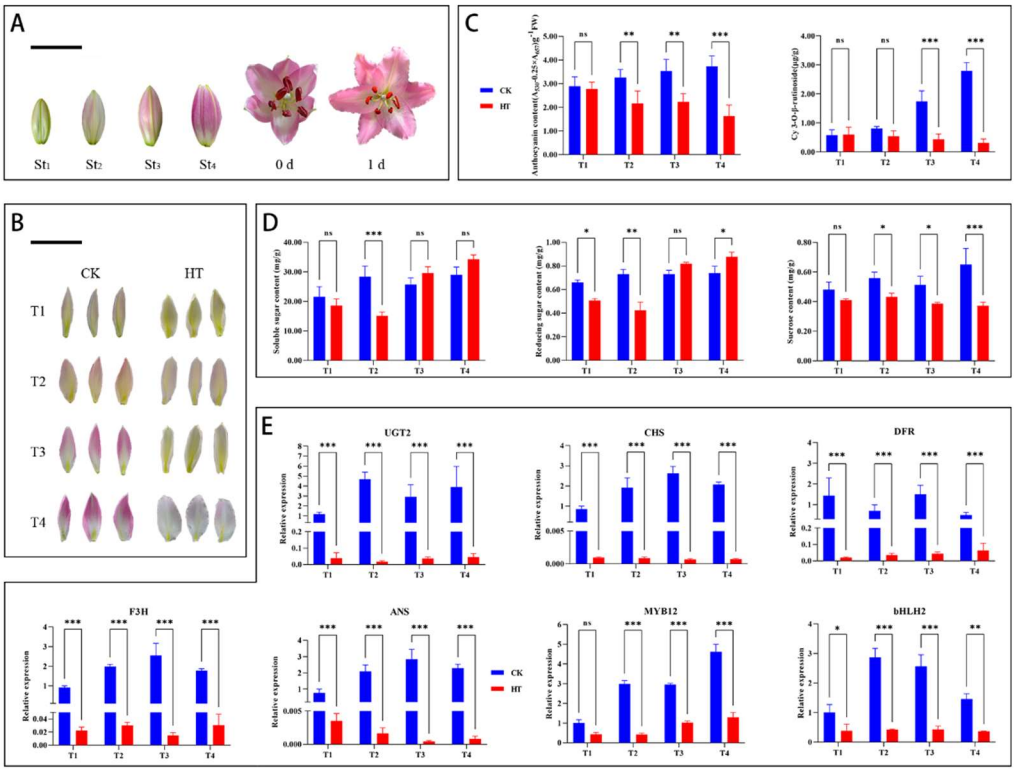

Figure 1. (A) Diagram of the developmental stages of lilies. (B) Comparison of the color of the lily 'Souvenir' petals under different durations of high-temperature treatments T1, T2, T3, and T4. (C) The total anthocyanin

 doi:10.20944/preprints202503.2014.v1

content of the lily 'Souvenir' petals under high-temperature treatments at T1, T2, T3, and T4. (D) The Cyanidin 3-O-β-rutinoside content of the lily 'Souvenir' petals under high-temperature treatments at T1, T2, T3, and T4 (* $p < 0.1$, ** $p < 0.01$, *** $p < 0.001$).

3.2. Gene Expression Differences between NT- and HT-Treated Oriental Lily

RNA-seq analysis of Oriental lily 'Souvenir' flowers subjected to 20°C and 35°C treatments (collected at four time points) generated 143.9 Gb of high-quality clean data with Q30 > 94.25%. In the absence of a reference genome for *Lilium* Oriental, clean reads were de novo assembled using Trinity software, yielding 63,394 Unigenes with an N50 length of 1.58 kb. Among these, 18,504 Unigenes exceeded 1 kb in length. Comprehensive functional annotation against multiple databases successfully classified 31,101 Unigenes (49.06%), with transcript abundance quantified using FPKM values. Differential expression analysis identified 8,354 differentially expressed genes (DEGs) across four pairwise comparisons ($|\log_2 FC| > 1$, adjusted $p < 0.01$). As illustrated in Figure 2A, the 35°C vs. 20°C comparison revealed distinct temporal expression patterns: at T1, 1,665 genes were up-regulated and 1,055 down-regulated; at T2, 1,581 genes showed up-regulation while 1,107 exhibited down-regulation; at T3, 1,885 genes were up-regulated and 1,854 down-regulated; and at T4, 1,946 genes displayed increased expression while 1,957 showed decreased expression. The Venn diagram analysis (Figure 2B) revealed 738 DEGs consistently differentially expressed across all four time points (T1, T2, T3, and T4; corresponding to 12, 24, 48, and 72 hours post-temperature treatment). Notable time-specific expression patterns were observed, with 931, 569, 684, and 892 unique DEGs identified at T1, T2, T3, and T4, respectively. This temporal diversity in transcriptional profiles indicates a sophisticated and dynamic gene expression reprogramming in response to elevated temperature stress over time.

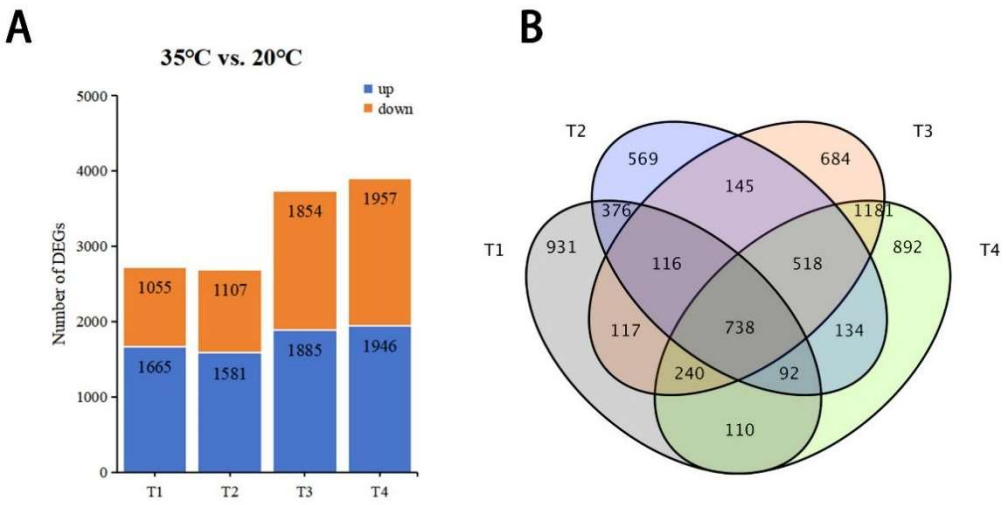

Figure 2. Histogram and Venn diagram showing numbers of differentially expressed genes (DEGs) in the comparisons 35 °C vs. 20 °C at T1, T2, T3, and T4. (A) Histogram showing numbers of up- and down-regulated DEGs in the comparisons 35 °C vs. 20 °C at T1, T2, T3, and T4. (B) Venn diagram presenting the overlap of DEGs in the comparisons 35 °C vs. 20 °C at T1, T2, T3, and T4. T1, T2, T3, and T4 represent oriental lily after 12, 24, 48, and 72 hours of 20 °C and 35 °C treatment, respectively.

3.3. Functional Classification of DEGs

GO and KEGG pathway analyses were performed to understand the biological functions of DEGs across different time points. GO analysis revealed a dynamic response pattern to high-temperature stress (Figure 3). At T1, biological processes were predominantly enriched in stress response terms, including 'response to hydrogen peroxide', 'response to reactive oxygen species',

 doi:10.20944/preprints202503.2014.v1

and 'response to heat' ($-\log_{10}$(p-value) > 12.5), indicating the activation of immediate stress response mechanisms. The cellular component analysis showed significant enrichment in membrane system terms, particularly 'integral component of membrane'. At T2, RNA modification emerged as the most significantly enriched term ($-\log_{10}$(p-value) = 25), while stress response pathways remained active. Notably, cellular components showed substantial changes in 'intracellular membrane-bounded organelle' and organelle-related terms. By T3, the enriched terms shifted towards light response and protection mechanisms, with significant enrichment in 'photoprotection' and 'cellular response to red light', suggesting adaptation of photosynthetic machinery. At T4, 'RNA modification' and 'mitochondrial mRNA processing' became prominently enriched, accompanied by metabolic regulation terms.

Based on the results of KEGG enrichment analysis, we can clearly observe distinct temporal patterns in metabolic and signaling pathway responses (Figure 4). In the early phase (T1), protein processing in the endoplasmic reticulum pathway was significantly enriched, reflecting how plant cells initially respond to heat damage through protein quality control mechanisms. As stress continued to 24 hours (T2), secondary metabolism-related pathways, particularly flavonoid biosynthesis, began to show significant responses, indicating a transition from immediate protective mechanisms to metabolic adjustment phases. By 48-72 hours (T3-T4), plant-pathogen interaction pathways and defense-related mechanisms became more prominent, while anthocyanin biosynthesis showed specific enrichment at T3, directly correlating with the observed decrease in pigment content. Notably, the plant hormone signal transduction pathway maintained a consistent moderate level of enrichment throughout the stress process, suggesting that hormone signaling plays a continuous regulatory role in coordinating heat stress responses. This temporal metabolic network reorganization reveals the complex adaptation mechanisms of lilies to high temperature stress, involving a complete process from protein homeostasis maintenance to metabolic adjustment and defense system activation. These findings provide important clues for understanding the regulatory network of pigment synthesis, supporting our identification of *LhERF109* as a key regulatory factor connecting heat stress response and anthocyanin biosynthesis.

 doi:10.20944/preprints202503.2014.v1

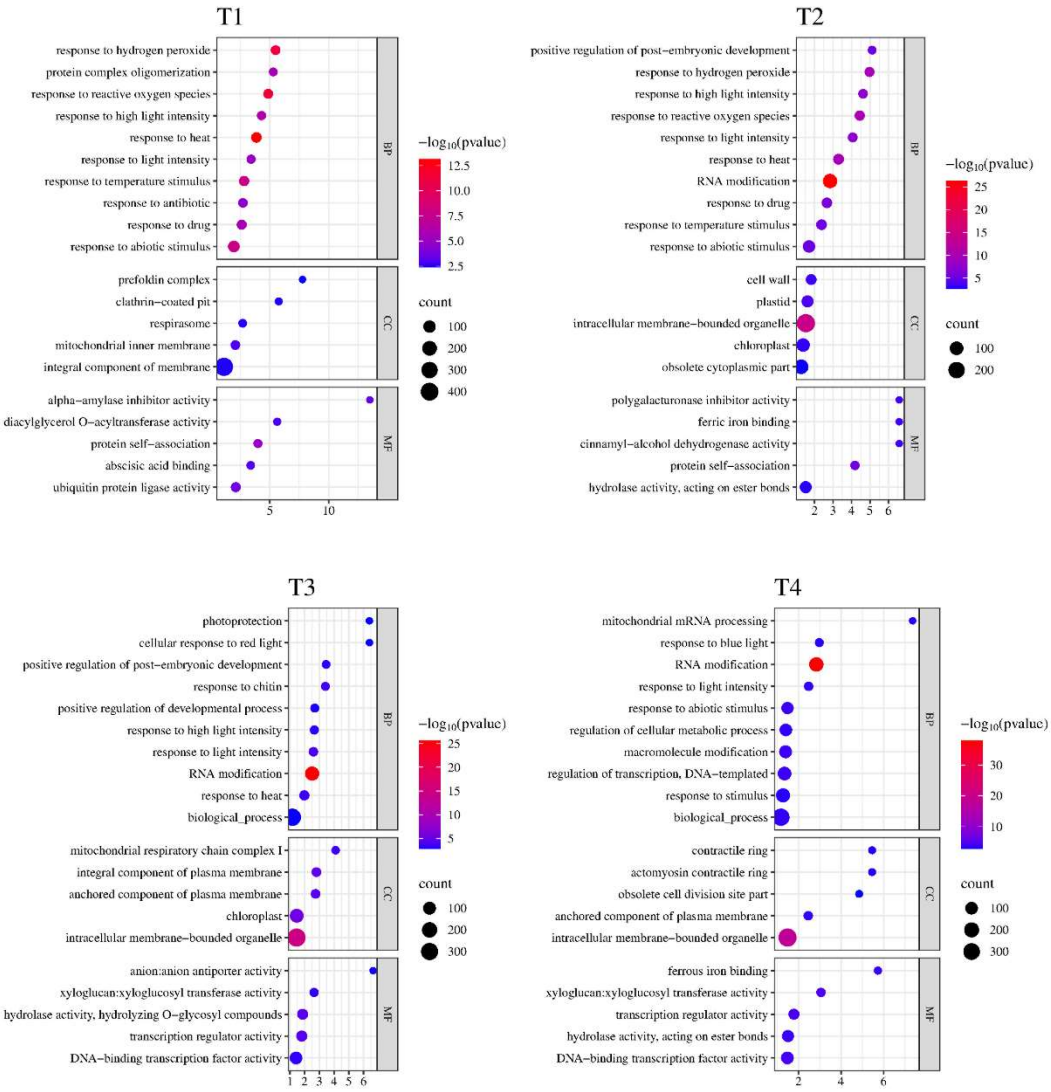

Figure 3. Gene Ontology (GO) enrichment analysis of differentially expressed genes (DEGs) in Oriental lily tepals under high temperature stress. The DEGs were categorized into three main types: biological process (BP), cellular component (CC), and molecular function (MF). T1, T2, T3, and T4 represent samples collected at 3, 6, 9, and 12 days after 20°C and 35°C treatment, respectively. The color scale indicates -log10(p-value) of enriched GO terms, and the size of dots represents the count of genes in each term.

 doi:10.20944/preprints202503.2014.v1

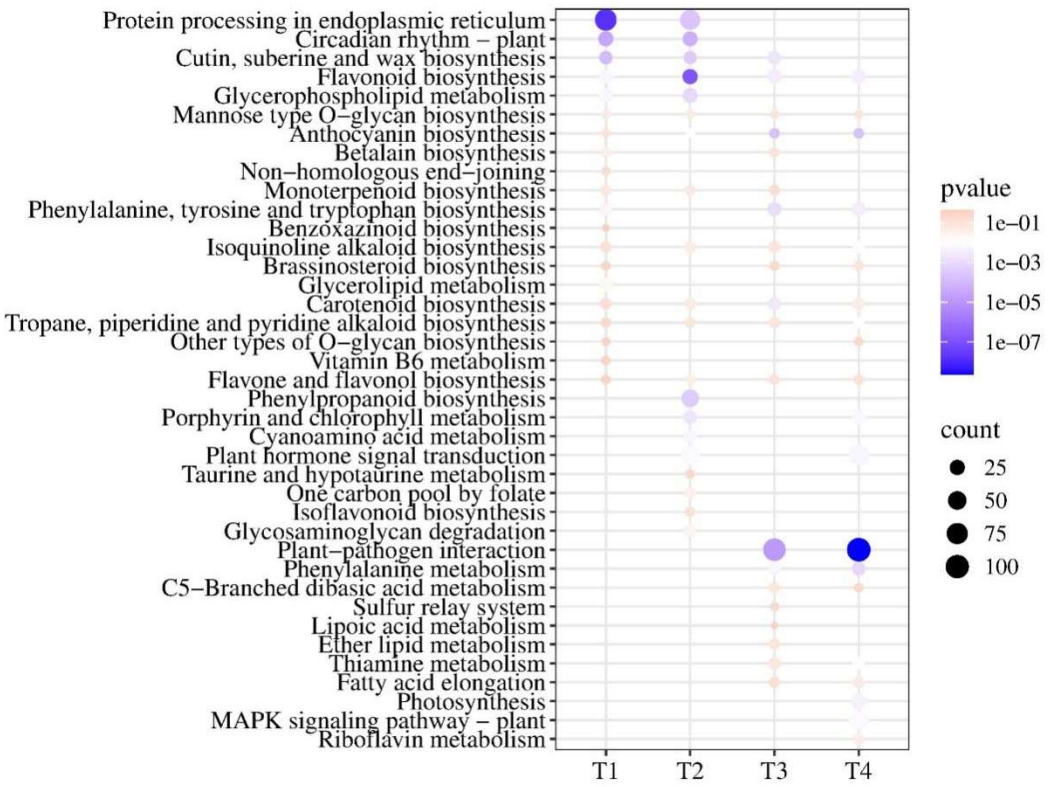

Figure 4. KEGG pathway enrichment analysis of differentially expressed genes (DEGs) in Oriental lily tepals at 35 °C vs. 20 °C comparisons at T1, T2, T3, and T4. T1, T2, T3, and T4 represent tepals after 12h, 24h, 48h, and 72h of temperature treatment, respectively.

3.4. Anthocyanin-Related DEGs Revealed by Analysis of Co-Expression Networks

The weighted gene co-expression network analysis (WGCNA) resulted in the identification of eight distinct co-expression modules (Figure 5A and 5B). Among these eight modules, the black module (MEblack) exhibited the strongest positive correlations with cyanidin-3-rutinoside (cy-3) and total anthocyanin content (TCA) (correlation coefficients of 0.9 and 0.69, respectively, $P<0.01$), suggesting that genes within this module likely play crucial roles in anthocyanin accumulation under temperature stress. The gene co-expression network was constructed using known anthocyanin-related genes, including the key transcription factor MYB12 and structural genes involved in the anthocyanin biosynthetic pathway (ANS, DFR, UGT78, and F3'H), along with potential regulatory transcription factors identified in the black module (Figure 5C). Network topology analysis revealed that MYB12 exhibited high connectivity with several structural genes and other transcription factors, serving as a central hub gene in the network. The structural genes, particularly ANS and DFR, showed strong connections with multiple transcription factors, including members of the ERF, NAC, and BHLH families, suggesting complex regulatory mechanisms controlling anthocyanin biosynthesis under temperature stress. Network visualization was conducted using Cytoscape with a weight threshold of 0.95.

The gene expression heatmap (Figure 5D) further corroborated these findings, showing significant differences in gene expression patterns between 20°C and 35°C treatments. Most genes in the black module, including MYB12, ANS, DFR, and F3'H, exhibited higher expression levels at 20°C and significantly decreased expression at 35°C, consistent with the trends observed in anthocyanin content. Notably, several transcription factors from the ERF, NAC, and WRKY families displayed temperature-sensitive expression patterns, indicating their potential roles as key regulators of temperature-responsive anthocyanin synthesis.

Overall, our WGCNA analysis established a comprehensive co-expression network centered around known anthocyan in biosynthetic genes and identified key regulatory transcription factors

 doi:10.20944/preprints202503.2014.v1

associated with temperature-dependent anthocyanin accumulation, providing important candidate genes for further functional validation.

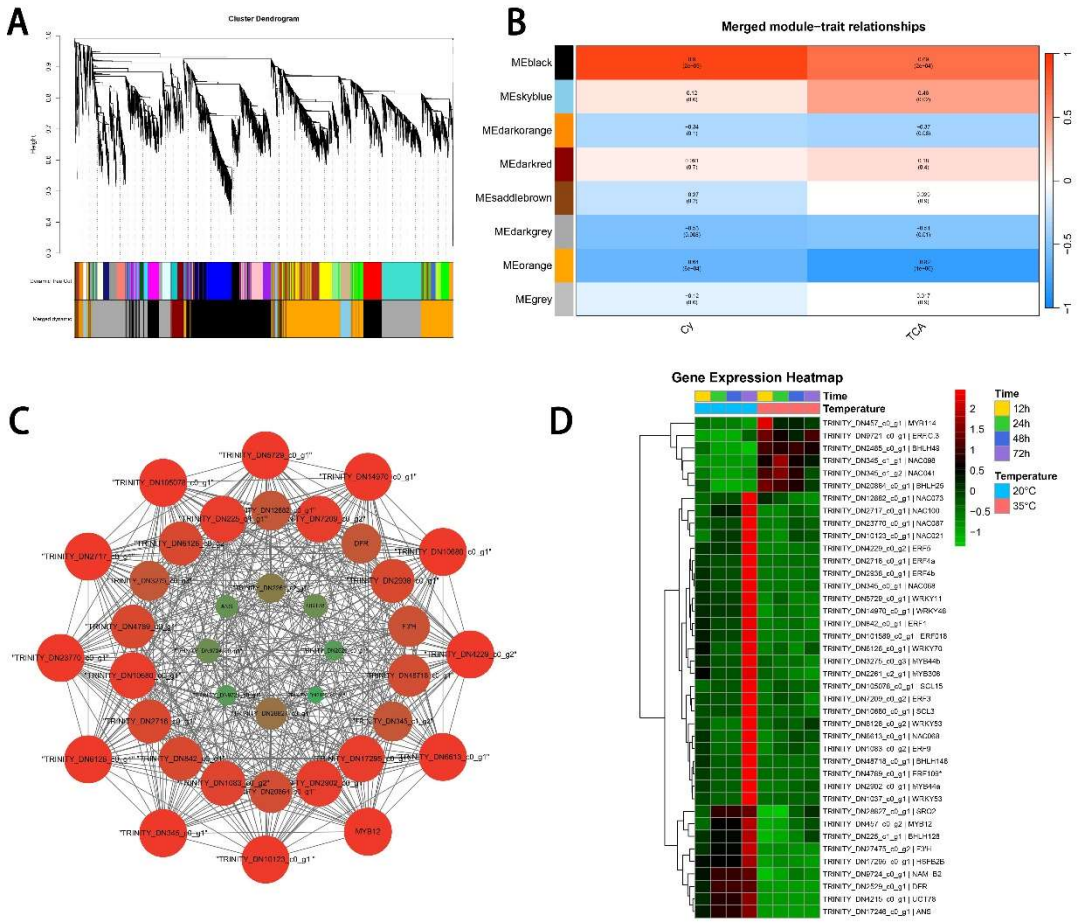

Figure 5. Weighted gene co-expression network analysis (WGCNA) of DEGs in apple at 20°C and 35°C treatment. (A) Hierarchical cluster tree presenting modules of co-expressed genes with color annotation. (B) Module–anthocyanin correlations and corresponding p-values. (C) Connection network between 5 anthocyanin structural genes and 21 TFs (transcript factors) in the 'black' module. (D) The heat map for the expression of 12 anthocyanin structural genes and 21 TFs (transcript factors) in the 'black' module.

3.5. Phylogenetic Tree Construction of LhERF109

Phylogenetic analysis positioned *LhERF109* within ERF subfamily Group X, clustering with *AtERF109* (At4g34410) with high bootstrap support (92%) (Figure 6A).

LhERF109 plays a critical role in regulating anthocyanin biosynthesis in Oriental lily 'Souvenir'. Compared with the control (S1300), transient overexpression of *LhERF109* (*LhERF109*-S1300) significantly enhanced anthocyanin accumulation in tepals, resulting in deeper purple-red pigmentation (Figure 7A). Conversely, silencing of *LhERF109* (*LhERF109*-TRV) markedly reduced anthocyanin accumulation, leading to lighter coloration compared to the TRV control (Figure 7A). Quantitative RT-PCR confirmed the successful overexpression and silencing of *LhERF109* in the respective treatments (Figure 7B).

Consistent with the phenotypic changes, anthocyanin biosynthetic genes showed differential expression patterns across treatments. Early and middle-stage genes including *LhMYB12*, *LhWD40a*, *LhCHSb*, and *LhANS* were significantly upregulated in *LhERF109*-S1300 compared to the control, while they were downregulated in the *LhERF109*-TRV treatment (Figure 7C). Notably, *LhBHLH2* expression remained relatively stable in the overexpression treatment but was significantly reduced in the silenced group.

 doi:10.20944/preprints202503.2014.v1

For late-stage and transport-related genes, most followed a similar pattern, with *LhUGT2*, *LhUGT3*, and *LhGSTF10* showing strong upregulation in *LhERF109*-S1300 and downregulation in *LhERF109*-TRV (Figure 7D). Interestingly, *LhF3H* displayed an opposite regulation pattern, being downregulated in *LhERF109*-S1300 and upregulated in *LhERF109*-TRV. *LhDFR* exhibited unique behavior with upregulation in both overexpression and silencing treatments, though through potentially different mechanisms. *LhF3'H* showed minimal response to *LhERF109* manipulation, suggesting alternative regulatory control.

These results demonstrate that *LhERF109* functions as a positive regulator of anthocyanin biosynthesis in Oriental lily by modulating the expression of key structural and regulatory genes in the anthocyanin pathway, with gene-specific regulatory patterns that suggest a complex control network.

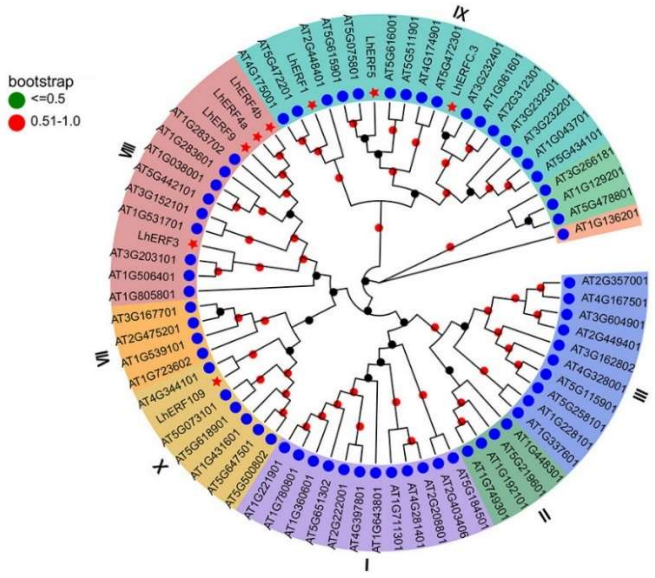

Figure 6. Phylogenetic analysis of ERF transcription factors from *Lilium* and *Arabidopsis thaliana*.

 doi:10.20944/preprints202503.2014.v1

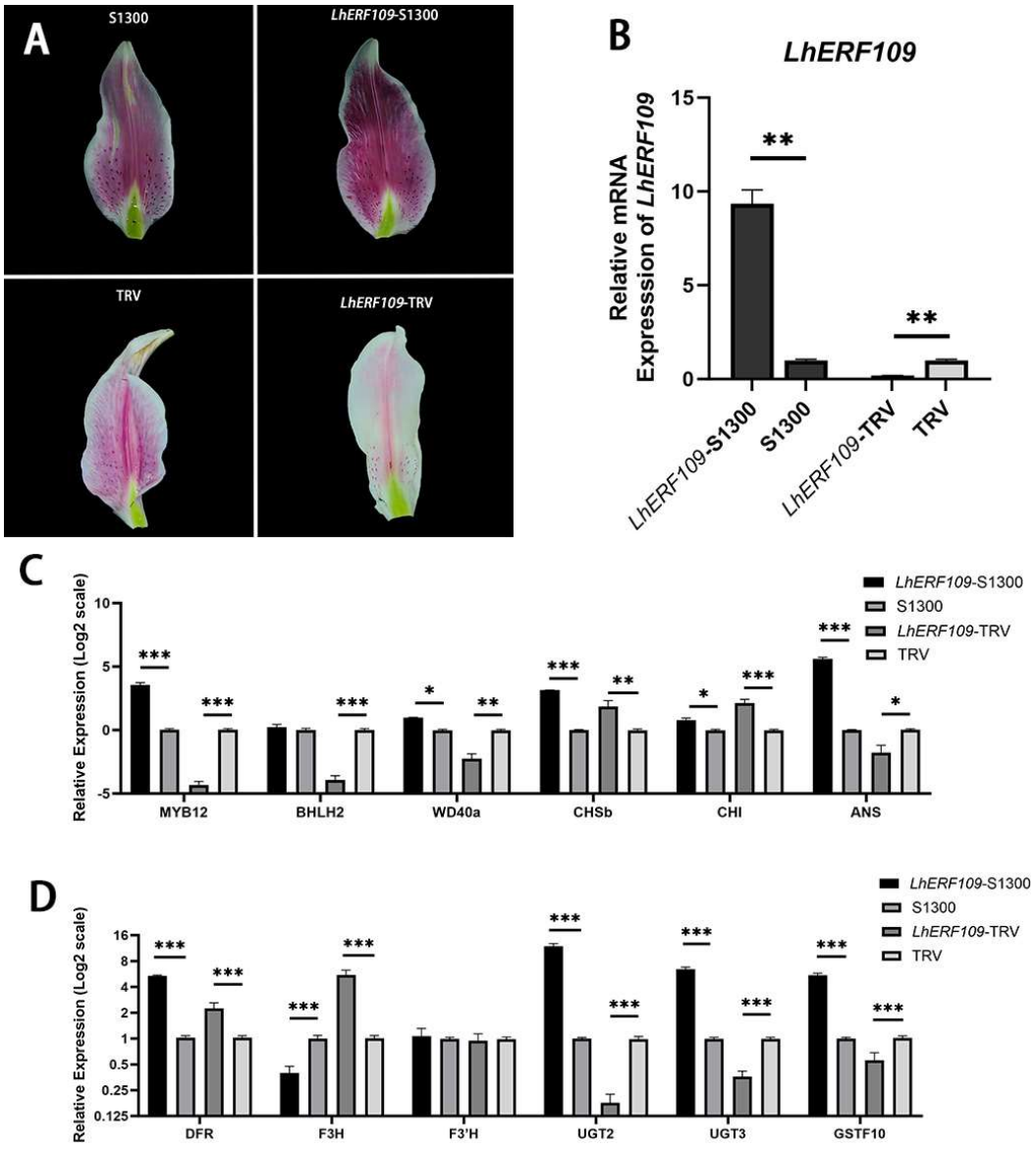

Figure 7. *LhERF109*-regulated anthocyanin biosynthesis in Oriental lily 'Souvenir'. (A) The phenotypes of S1300, *LhERF109*-S1300, TRV, and *LhERF109*-TRV lily tepals. (B) The expression levels of *LhERF109* in S1300, *LhERF109*-S1300, TRV, and *LhERF109*-TRV treatments. (C) The expression levels of early and middle-stage anthocyanin biosynthesis genes in S1300, *LhERF109*-S1300, TRV, and *LhERF109*-TRV treatments. (D) The expression levels of late-stage anthocyanin biosynthesis and transport-related genes in S1300, *LhERF109*-S1300, TRV, and *LhERF109*-TRV treatments. Values represent means ± SD of three independent biological replicates. Statistical significance was computed with the use of Student's t-test (* $p < 0.1$, ** $p < 0.01$, *** $p < 0.001$).

4. Discussion

High temperature significantly inhibits anthocyanin accumulation in plant tissues, but the regulatory mechanisms differ among species and tissues [13]. Our transcriptome analysis of Oriental lily tepals under heat stress revealed a complex metabolic network reconstruction. KEGG analysis showed that protein processing in endoplasmic reticulum was most significant in the T1 stage, while flavonoid biosynthesis, anthocyanin biosynthesis, and phenylpropanoid metabolism were continuously enriched from T2 to T4 stages. In addition, circadian rhythm, plant hormone signal transduction, and chlorophyll metabolism pathways also showed significant enrichment. The GO enrichment analysis further revealed a progressive transition from early stress response (ROS-related terms) to later metabolic adaptation (membrane system modifications) in lily tepals. This temporal pattern differs from what has been observed in apple fruits, where carbon metabolism was

 doi:10.20944/preprints202503.2014.v1

consistently the most enriched pathway [8,35]. Our findings also contrast with observations in grape berries, where heat stress primarily affects flavonoid pathway genes through direct transcriptional suppression [36]. In the chrysanthemum study, functional annotation and enrichment analysis revealed significant enrichment of heat shock response and flavonoid biosynthesis pathways, with 63 differentially expressed genes associated with 'flavonoid biosynthesis' highlighting the temperature sensitivity of this pathway [37]. These multi-species comparisons suggest that the regulation of heat-induced anthocyanin accumulation varies significantly among different species.

High temperature stress significantly affects sugar metabolism and anthocyanin synthesis in the petals of Oriental lily 'Souvenir'. Our research demonstrates that under high temperature conditions, sucrose content consistently decreases while soluble sugars show a dynamic pattern of initial decrease followed by increase, which aligns with the significant enrichment of heat response and abiotic stress response pathways in GO analysis. Sucrose, serving as both a precursor and signaling molecule for anthocyanin synthesis, directly influences anthocyanin accumulation [38,39]. Heat stress disrupts the normal relationship between sucrose and anthocyanin synthesis, leading to significant inhibition of anthocyanin biosynthesis. The accumulation of soluble sugars serves as a protective mechanism to regulate osmotic pressure and lower metabolic rates under high temperature [40,41]. These findings provide insights for enhancing plant heat tolerance through exogenous sugar applications [42,43].

Recent research by Yang et al. [4] suggests that heat stress redirects metabolic resources from anthocyanin biosynthesis toward isoflavone synthesis in lily petals. However, our results challenge this interpretation. Our analysis revealed that total anthocyanin content significantly decreases under high temperature (35°C), with cyanidin, a major anthocyanin in lily tepals, showing particularly severe suppression compared to normal conditions (20°C). This overall reduction in anthocyanin content indicates that multiple mechanisms beyond simple metabolic redirection are involved in the heat response. This pattern resembles findings in cereal crops, where heat stress triggers coordinated adjustments in primary metabolism, hormone signaling, and secondary metabolite production [44]. These findings highlight the importance of species-specific approaches in heat tolerance breeding.

Through WGCNA analysis and co-expression network construction within the black module, we successfully identified *LhERF109* as a key regulator associated with anthocyanin-related genes. Based on comprehensive evidence across multiple species and our experimental findings, we propose that *LhERF109* functions as a critical molecular integrator connecting heat stress responses with anthocyanin biosynthesis in Oriental lily. Phylogenetic analysis positions *LhERF109* within the Group X ERF subfamily, clustering closely with Arabidopsis *AtERF109* with high bootstrap support (92%), indicating evolutionary conservation with Group IX ERFs, which are known to mediate stress responses and hormone signaling pathways such as jasmonic acid (JA), indole-3-acetic acid (IAA), and ethylene (ETH) [45–49]. Transient transformation experiments demonstrated that *LhERF109* overexpression (*LhERF109*-S1300) significantly enhanced tepal anthocyanin accumulation, evidenced by deeper purple-red pigmentation (Figure 7A), with robust upregulation of the regulatory gene *LhMYB12* and structural genes including *LhCHSb, LhDFR, LhUGT2, LhUGT3, and LhGSTF10, as well as LhANS* (Figure 7C, D). In contrast, silencing (*LhERF109*-TRV) resulted in lighter coloration and reduced anthocyanin content, accompanied by significant downregulation of *LhMYB12, LhBHLH2, LhWD40a*, *LhUGT2*, *LhUGT3*, *LhGSTF10*, and *LhANS* (Figure 7A, C, D). The expression of *LhBHLH2* exhibited an asymmetric pattern, remaining stable during overexpression but significantly downregulated upon silencing (Figure 7C), suggesting a complex regulatory mechanism beyond simple transcriptional activation.

The pronounced upregulation of *LhANS* during overexpression suggests that *LhERF109* may directly target anthocyanin biosynthesis genes, enhancing the conversion of leucoanthocyanidins to anthocyanidins, a rate-limiting step in anthocyanin biosynthesis. Notably, the significant induction of late-stage anthocyanin biosynthesis genes, particularly transport-related genes such as *LhUGT2*, *LhUGT3*, and *LhGSTF10*, suggests that *LhERF109* may play a critical role in facilitating anthocyanin transport and stabilization under heat stress conditions. This regulatory mechanism is supported by

 doi:10.20944/preprints202503.2014.v1

similar observations in other species, such as *MdERF1B* in apple, which binds MdANS and *MdUFGT* promoters [47], and MdERF38, which interacts with *MdDFR* and *MdUFGT* under drought stress [50].

The asymmetric regulation of *LhBHLH2*, with minimal upregulation during overexpression and significant downregulation during silencing, mirrors patterns in other species. In apple, *MdMYB10* overexpression strongly activates *MdUFGT* with little effect on *MdBHLH33*, whereas RNAi silencing significantly downregulates *MdBHLH33* [50]. In grape, *VvMYBA1* overexpression promotes *VvUFGT* with stable *VvBHLH1*, while silencing markedly reduces *VvBHLH1* [51]. Similarly, in petunia, *PhMYB27* overexpression enhances anthocyanin with limited *PhBHLH3* upregulation, but silencing leads to a pronounced *PhBHLH3* reduction [52], and in Arabidopsis, *AtMYB75* overexpression induces DFR with minimal *AtBHLH42* (GL3) change, while silencing significantly downregulates *AtBHLH42* [53]. These parallels suggest that *LhERF109* may prioritize MYB and ANS-mediated activation under heat stress, while indirectly maintaining BHLH, a strategy potentially conserved across species.

In conclusion, our study demonstrates that ERF109, as a heat-responsive transcription factor, influences lily flower coloration by regulating multiple stages of the anthocyanin biosynthesis pathway. This finding not only enriches our understanding of plant color regulation but also provides potential molecular targets for breeding heat-resistant varieties with stable flower coloration. Future research should focus on the potential interaction mechanisms between ERF109 and the MBW complex, as well as how high temperatures affect ERF109 expression and activity, to further understand the temperature-transcription factor-color formation regulatory network.

5. Conclusion

This study reveals the molecular mechanisms of flower color changes in Oriental lily under heat stress through transcriptome analysis and Weighted Gene Co-expression Network Analysis (WGCNA). We found that high temperature inhibits anthocyanin accumulation, leading to color fading. Using WGCNA, we identified *LhERF109* as a key transcription factor regulating this process for the first time and verified its regulatory effects on critical anthocyanin biosynthesis genes. Transient transformation experiments demonstrated that *LhERF109* overexpression significantly enhanced tepal anthocyanin accumulation, while silencing resulted in lighter coloration and reduced anthocyanin content. Future research will focus on the precise mechanisms of *LhERF109*, providing support for breeding heat-tolerant ornamental crops with stable flower coloration.

Supplementary Materials: The following supporting information can be downloaded at the website of this paper posted on Preprints.org, Table1 and Table 2.

Author Contributions: M.Z. and L.Z.: writing-original draft, visualization, data curation, writing-review & editing. F. L. and C.J.: resources, supervision, methodology, writing-review & editing J.Z.: methodology. X.Y. and M.W.: validation, data curation, conceptualization. B.J. and Y.J.: supervision, investigation. H.J.: resources. J.W.: conceptualization, supervision, funding acquisition. Y.Z.: conceptualization, writing-review & editing, investigation, supervision, project administration, funding acquisition. All authors have read and agreed to the published version of the manuscript.

Funding: This work was supported by the Natural Science of Sichuan Province (grant number 2023NSFSC0139), Sichuan Province '14th Five-Year Plan' Breeding Research Project (grant number 2021YFYZ0006), Yunnan Xingdian Talents—Special Selection Project for High-level Scientific and Technological Talents and Innovation Teams-Team Specific Project (202505AS350021), High-level Talent Introduction Program of Yunnan Province—Industrial Talent Special Project (YNQR-CYRC-2020-004) and Yunnan Xingdian Talents—Youth Special Project (XDYC-QNRC-2022-0731).

Data Availability Statement: The raw data supporting the conclusions of this article will be made available by the authors on request.

Conflicts of Interest: The authors have no conflicts of interest to declare.

 doi:10.20944/preprints202503.2014.v1

References

1. Lu, Z.; Wang, X.; Lin, X.; Mostafa, S.; Zou, H.; Wang, L.; Jin, B. Plant anthocyanins: Classification, biosynthesis, regulation, bioactivity, and health benefits. Plant Physiol. Biochem. **2024**, 217, 109268.
2. Manzoor, M.A.; Xu, Y.; lv, Z.; Xu, J.; Shah, I.H.; Sabir, I.A.; Wang, Y.; Sun, W.; Liu, X.; Wang, L.; Liu, R.; Jiu, S.; Zhang, C. Horticulture crop under pressure: Unraveling the impact of climate change on nutrition and fruit cracking. J. Environ. Manage. **2024**, 357, 120759.
3. Yamagishi, M.; Nakatsuka, T. *LhMYB12*, Regulating Tepal Anthocyanin Pigmentation in Asiatic Hybrid Lilies, is Derived from Lilium dauricum and L. bulbiferum. Hortic. J. **2017**, 86, 528–33.
4. Yang, J.; Guo, C.; Chen, F.; Lv, B.; Song, J.; Ning, G.; He, Y.; Lin, J.; He, H.; Yang, Y.; Xiang, F. Heat-induced modulation of flavonoid biosynthesis via a *LhMYBC2*-Mediated regulatory network in oriental hybrid lily. Plant Physiol. Biochem. **2024**, 214, 108966.
5. Mori, K.; Goto-Yamamoto, N.; Kitayama, M.; Hashizume, K. Loss of anthocyanins in red-wine grape under high temperature. J. Exp. Bot. **2007**, 58, 1935–45.
6. Lin-Wang, K.; Micheletti, D.; Palmer, J.; Volz, R.; Lozano, L.; Espley, R.; Hellens, R.P.; Chagnè, D.; Rowan, D.D.; Troggio, M.; Iglesias, I.; Allan, A.C. High temperature reduces apple fruit colour via modulation of the anthocyanin regulatory complex. Plant Cell Environ. **2011**, 34, 1176–90.
7. Rowan, D.D.; Cao, M.; Lin-Wang, K.; Cooney, J.M.; Jensen, D.J.; Austin, P.T.; Hunt, M.B.; Norling, C.; Hellens, R.P.; Schaffer, R.J.; Allan, A.C. Environmental regulation of leaf colour in red 35S *Arabidopsis thaliana*. New Phytol. **2009**, 182, 102–15.
8. Rehman, R.N.U.; You, Y.; Zhang, L.; Goudia, B.D.; Khan, A.R.; Li, P.; Ma, F. High Temperature Induced Anthocyanin Inhibition and Active Degradation in *Malus* profusion. Front. Plant Sci. **2017**, 8, 1401.
9. Bai, S.; Tao, R.; Tang, Y.; Yin, L.; Ma, Y.; Ni, J.; Yan, X.; Yang, Q.; Wu, Z.; Zeng, Y.; Teng, Y. *BBX16*, a B-box protein, positively regulates light-induced anthocyanin accumulation by activating MYB10 in red pear. Plant Biotechnol. J. **2019**, 17, 1985–97.
10. Fang, H.; Dong, Y.; Yue, X.; Hu, J.; Jiang, S.; Xu, H.; Wang, Y.; Su, M.; Zhang, J.; Zhang, Z.; Wang, N.; Chen, X. The B-box zinc finger protein *MdBBX20* integrates anthocyanin accumulation in response to ultraviolet radiation and low temperature. Plant Cell Environ. **2019**, 42, 2090–104.
11. Kim, S.; Hwang, G.; Lee, S.; Zhu, J-Y.; Paik, I.; Nguyen, T.T.; Kim, J.; Oh, E. High Ambient Temperature Represses Anthocyanin Biosynthesis through Degradation of HY5. Front. Plant Sci. **2017**, 8, 1787.
12. Nguyen, N.H. HY5, an integrator of light and temperature signals in the regulation of anthocyanins biosynthesis in Arabidopsis. AIMSMOLES **2020**, 7, 70–81.
13. Yamagishi, M. Mechanisms by Which High Temperatures Suppress Anthocyanin Coloration in Flowers and Fruits, and Discovery of Floricultural Crops that Exhibit High-temperature-tolerant Flower Pigmentation. Hortic. J. **2024**, 93, 203–15.
14. Liu, Z.; Zhang, Y.; Wang, J.; Li, P.; Zhao, C.; Chen, Y.; Bi, Y. Phytochrome-interacting factors PIF4 and PIF5 negatively regulate anthocyanin biosynthesis under red light in Arabidopsis seedlings. Plant Sci. **2015**, 238, 64–72.
15. Li, Y.; Shan, X.; Gao, R.; Han, T.; Zhang, J.; Wang, Y.; Kimani, S.; Wang, L.; Gao, X. MYB repressors and MBW activation complex collaborate to fine-tune flower coloration in Freesia hybrida. Commun. Biol. **2020**, 3, 1–14.
16. Li, Z.; Zhou, H.; Chen, Y.; Chen, M.; Yao, Y.; Luo, H.; Wu, Q.; Wang, F.; Zhou, Y. Analysis of Transcriptional and Metabolic Differences in the Petal Color Change Response to High-Temperature Stress in Various Chrysanthemum Genotypes. Agronomy **2024**, 14, 2863.
17. An, W.; Sun, Y.; Gao, Z.; Liu, X.; Guo, Q.; Sun, S.; Zhang, M.; Han, Y.; Irfan, M.; Chen, L.; Ma, D. LvbHLH13 Regulates Anthocyanin Biosynthesis by Activating the *LvMYB5* Promoter in Lily (*Lilium* 'Viviana'). Horticulturae **2024**, 10, 926.
18. Wang, N.; Song, G.; Zhang, F.; Shu, X.; Cheng, G.; Zhuang, W.; Wang, T.; Li, Y.; Wang, Z. Characterization of the WRKY Gene Family Related to Anthocyanin Biosynthesis and the Regulation Mechanism under Drought Stress and Methyl Jasmonate Treatment in Lycoris radiata. Int. J. Mol. Sci. **2023**, 24, 2423.
19. Xie, Z.; Nolan, T.M.; Jiang, H.; Yin, Y. AP2/ERF Transcription Factor Regulatory Networks in Hormone and Abiotic Stress Responses in Arabidopsis. Front. Plant Sci. **2019**, 10, 1177.

 doi:10.20944/preprints202503.2014.v1

20. Zhang, S.; Chen, Y.; Zhao, L.; Li, C.; Yu, J.; Li, T.; Yang, W.; Zhang, S.; Su, H.; Wang, L. A novel NAC transcription factor, *MdNAC42*, regulates anthocyanin accumulation in red-fleshed apple by interacting with MdMYB10. Tree Physiol. **2020**, 40, 413–23.
21. Zhang, Y.; Sun, Y.; Du, W.; Sun, S.; Zhang, S.; Nie, M.; Liu, Y.; Irfan, M.; Zhang, L.; Chen, L. Ethylene positively regulates anthocyanin synthesis in "Viviana" lily via the *LvMYB5-LvERF113-LvMYB1* module. Hortic. Res. **2025**.
22. Zhang, X.; Yu, L.; Zhang, M.; Wu, T.; Song, T.; Yao, Y.; Zhang, J.; Tian, J. MdWER interacts with *MdERF109* and *MdJAZ2* to mediate methyl jasmonate- and light-induced anthocyanin biosynthesis in apple fruit. Plant J. **2024**, 118, 1327–42.
23. Grassotti, A.; Gimelli, F. Bulb and cut flower production in the genus *Lilium*: Current status and the future. Acta Hortic. **2011**, 900, 21–35.
24. Van Tuyl, J.M.; Arens, P. *Lilium*: Breeding history of the modern cultivar assortment. Acta Hortic. **2011**, 900, 223–30.
25. Natenapit, J.; Taketa, S.; Narumi, T.; Fukai, S. Crossing of Allotriploid LLO Hybrid and Asiatic Lilies (*Lilium*). Hortic. Environ. Biotechnol. **2010**, 51, 426–30.
26. Barba-Gonzalez, R.; Van Silfhout, A.A.; Visser, R.G.F.; Ramanna, M.S.; Van Tuyl, J.M. Progenies of allotriploids of Oriental × Asiatic lilies (*Lilium*) examined by GISH analysis. Euphytica **2006**, 151, 243–50.
27. Zhou, M.; Yong, X.; Zhu, J.; Xu, Q.; Liu, X.; Zhang, L.; Mou, L.; Zeng, L.; Wu, M.; Jiang, B.; Jia, Y.; Zhang, P.; Pan, Y. Chromosomal analysis of progenies between *Lilium i*ntersectional hybrids and wild species using ND-FISH and GISH. Front. Plant Sci. **2024**, 15, 1274883.
28. Lai, Y-S.; Yamagishi, M.; Suzuki, T. Elevated temperature inhibits anthocyanin biosynthesis in the tepals of an Oriental hybrid lily via the suppression of *LhMYB12* transcription. Sci. Hortic. **2011**, 132, 59–65.
29. Song, X.; Yang, Q.; Liu, Y.; Li, J.; Chang, X.; Xian, L.; Zhang, J. Genome-wide identification of Pistacia R2R3-MYB gene family and function characterization of *PcMYB113* during autumn leaf coloration in Pistacia chinensis. Int. J. Biol. Macromol. **2021**, 192, 16–27.
30. Xia, H.; Liu, X.; Jiang, G.Z.; Liu, P.; Ji, L.X. Establishment of High Performance Liquid Chromatography Method for Determination of Cyanidin-3-O-glucoside in Black Rice Anthocyanins. Grain Food Ind. **2024**, 31, 68–72.
31. Zhang, S.; Luo, Z.; Wu, X.; Shi, B.; Jiang, H.; Zhou, L.; Bai, L. Comparative Transcriptomic Analysis of Root Cadmium Responses in Two Chinese Rice Cultivars Yuzhenxiang and Xiangwanxian 12. J. Chem. **2021**, 2021, 2166775.
32. Dou, H.; Wang, T.; Zhou, X.; Feng, X.; Tang, W.; Quan, J.; Bi, H. Genome-Wide Identification and Expression of the AP2/ERF Gene Family in Morus notabilis. Forests **2024**, 15, 697.
33. Yin, X.; Zhang, Y.; Zhang, L.; Wang, B.; Zhao, Y.; Irfan, M.; Chen, L.; Feng, Y. Regulation of MYB Transcription Factors of Anthocyanin Synthesis in Lily Flowers. Front. Plant Sci. **2021**, 12, 699303.
34. Gao, J.; Li, W-B.; Liu, H-F.; Chen, F-B. De novo transcriptome sequencing of radish (Raphanus sativus L.) fleshy roots: analysis of major genes involved in the anthocyanin synthesis pathway. BMC Mol. Cell Biol. **2019**, 20, 45.
35. Bu, Y-F.; Wang, S.; Li, C-Z.; Fang, Y.; Zhang, Y.; Li, Q-Y.; Wang, H-B.; Chen, X-S.; Feng, S-Q. Transcriptome Analysis of Apples in High-Temperature Treatments Reveals a Role of *MdLBD37* in the Inhibition of Anthocyanin Accumulation. Int. J. Mol. Sci. **2022**, 23, 3766.
36. Rienth, M.; Vigneron, N.; Darriet, P.; Sweetman, C.; Burbidge, C.; Bonghi, C.; Walker, R.P.; Famiani, F.; Castellarin, S.D. Grape Berry Secondary Metabolites and Their Modulation by Abiotic Factors in a Climate Change Scenario–A Review. Front. Plant Sci. **2021**, 12, 643258.
37. Shi, Z.; Han, X.; Wang, G.; Qiu, J.; Zhou, L.; Chen, S.; Fang, W.; Chen, F.; Jiang, J. Transcriptome analysis reveals chrysanthemum flower discoloration under high-temperature stress. Front. Plant Sci. **2022**, 13, 983292.
38. Solfanelli, C.; Poggi, A.; Loreti, E.; Alpi, A.; Perata, P. Sucrose-Specific Induction of the Anthocyanin Biosynthetic Pathway in Arabidopsis. Plant Physiol. **2006**, 140, 637–46.

 doi:10.20944/preprints202503.2014.v1

39. Liu, X-J.; An, X-H.; Liu, X.; Hu, D-G.; Wang, X-F.; You, C-X.; Hao, Y-J. MdSnRK1.1 interacts with MdJAZ18 to regulate sucrose-induced anthocyanin and proanthocyanidin accumulation in apple. J. Exp. Bot. **2017**, 68, 2977–90.
40. Yang, X.; Pang, X.; Xu, L.; Fang, R.; Huang, X.; Guan, P.; Lu, W.; Zhang, Z. Accumulation of soluble sugars in peel at high temperature leads to stay-green ripe banana fruit. J. Exp. Bot. **2009**, 60, 4051–62.
41. Tan, Y.; Wen, B.; Xu, L.; Zong, X.; Sun, Y.; Wei, G.; Wei, H. High temperature inhibited the accumulation of anthocyanin by promoting ABA catabolism in sweet cherry fruits. Front. Plant Sci. **2023**, 14, 1137826.
42. Ichimura, K.; Niki, T.; Matoh, M.; Nakayama, M. High temperature under low light conditions suppresses anthocyanin biosynthesis in snapdragon petals associated with decreased sugar levels. Sci. Hortic. **2021**, 290, 110510.
43. Liu, C.; Yu, H.; Liu, Y.; Zhang, L.; Li, D.; Zhao, X.; Zhang, J.; Sui, Y. Promoting Anthocyanin Biosynthesis in Purple Lettuce through Sucrose Supplementation under Nitrogen Limitation. Horticulturae **2024**, 10, 838.
44. Zhao, P.; Sun, L.; Zhang, S.; Jiao, B.; Wang, J.; Ma, C. Integrated Transcriptomics and Metabolomics Analysis of Two Maize Hybrids (ZD309 and XY335) under Heat Stress at the Flowering Stage. Genes **2024**, 15, 189.
45. Licausi, F.; Ohme-Takagi, M.; Perata, P. APETALA2/Ethylene Responsive Factor (AP2/ERF) transcription factors: mediators of stress responses and developmental programs. New Phytol. **2013**, 199, 639–49.
46. Cai, X-T.; Xu, P.; Zhao, P-X.; Liu, R.; Yu, L-H.; Xiang, C-B. Arabidopsis ERF109 mediates cross-talk between jasmonic acid and auxin biosynthesis during lateral root formation. Nat. Commun. **2014**, 5, 5833.
47. Zhang, J.; Xu, H.; Wang, N.; Jiang, S.; Fang, H.; Zhang, Z.; Yang, G.; Wang, Y.; Su, M.; Xu, L.; Chen, X. The ethylene response factor MdERF1B regulates anthocyanin and proanthocyanidin biosynthesis in apple. Plant Mol. Biol. **2018**, 98, 205–18.
48. Xu, P.; Zhao, P-X.; Cai, X-T.; Mao, J-L.; Miao, Z-Q.; Xiang, C-B. Integration of Jasmonic Acid and Ethylene Into Auxin Signaling in Root Development. Front. Plant Sci. **2020**, 11, 271.
49. Zhu, X.; Wang, B.; Liu, W.; Wei, X.; Wang, X.; Du, X.; Liu, H. Genome-wide analysis of AP2/ERF gene and functional analysis of CqERF24 gene in drought stress in quinoa. Int. J. Biol. Macromol. **2023**, 253, 127582.
50. An, J-P.; Zhang, X-W.; Bi, S-Q.; You, C-X.; Wang, X-F.; Hao, Y-J. The ERF transcription factor *MdERF38* promotes drought stress-induced anthocyanin biosynthesis in apple. Plant J. **2020**, 101, 573–89.
51. Kobayashi, S.; Goto-Yamamoto, N.; Hirochika, H. Retrotransposon-Induced Mutations in Grape Skin Color. Science **2004**, 304, 982–982.
52. Albert, N.W.; Davies, K.M.; Lewis, D.H.; Zhang, H.; Montefiori, M.; Brendolise, C.; Boase, M.R.; Ngo, H.; Jameson, P.E.; Schwinn, K.E. A Conserved Network of Transcriptional Activators and Repressors Regulates Anthocyanin Pigmentation in Eudicots. Plant Cell **2014**, 26, 962–80.
53. Gonzalez, A.; Zhao, M.; Leavitt, J.M.; Lloyd, A.M. Regulation of the anthocyanin biosynthetic pathway by the TTG1/bHLH/Myb transcriptional complex in Arabidopsis seedlings. Plant J. **2008**, 53, 814–27.